

CLINICAL RESEARCH ARTICLE



Early neonatal heart rate variability patterns in different subtypes of perinatal hypoxic-ischemic brain injury

Ipsita Goswami^{1✉}, Daphne Kamino², Elysa Widjaja³, Melissa Panicia⁴, Nicholas Mitsakakis⁵, Aideen Moore² and Emily W. Y. Tam²

© The Author(s), under exclusive licence to the International Pediatric Research Foundation, Inc 2022

BACKGROUND: This study aims to compare the longitudinal changes in heart rate variability (HRV) during therapeutic hypothermia in neonates with different subtypes of hypoxic-ischemic brain injury.

METHODS: HRV was computed from 1 hour time-epochs q6 hours for the first 48 hours. Primary outcome was brain-injury pattern on MRI at 4(3–5) days. We fitted linear mixed-effect regression models with HRV metric, brain injury subtype and postnatal age.

RESULTS: Among 89 term neonates, 40 neonates had abnormal brain MRI (focal infarct 15 (38%), basal-ganglia predominant 8 (20%), watershed-predominant 5 (13%), and mixed pattern 12 (30%). There was no significant difference in the HRV metrics between neonates with normal MRI, focal infarcts and basal ganglia pattern. At any given postnatal age, the degree of HRV suppression (HRV measure in the brain-injury subtype group/HRV measure in Normal MRI group) was significant in neonates with watershed pattern (SDNN(0.63, $p = 0.08$), RMSSD(0.74, $p = 0.04$)) and mixed pattern injury (SDNN (0.64, $p < 0.001$), RMSSD (0.75, $p = 0.02$)). HRV suppression was most profound at the postnatal age of 24–30 h in all brain injury subtypes.

CONCLUSION: Neonates with underlying watershed injury with or without basal-ganglia injury demonstrates significant HRV suppression during first 48 hour of hypothermia therapy.

Pediatric Research (2022) 92:1630–1639; <https://doi.org/10.1038/s41390-022-02016-9>

IMPACT:

- Our study suggests that suppression of heart rate variability in neonates during therapeutic hypothermia varies according to the pattern of underlying hypoxic-ischemic brain injury.
- Neonates with watershed predominant pattern and mixed pattern of brain injury have the most severe suppression of heart rate variability measures.
- Heart rate variability monitoring may provide early insights into the pattern of hypoxic-ischemic brain injury in neonates undergoing therapeutic hypothermia earlier than routine clinical MRI

INTRODUCTION

Therapeutic hypothermia improves survival and neurodevelopmental outcome following perinatal hypoxic-ischemic brain injury; however, almost 47% of infants will develop neurodeficits despite therapy^{1,2}. There is a need to optimize neuroprotective care by utilizing novel modalities for early clinical prognostication. Currently, the most reliable prognostic tool is the pattern of brain injury detected by conventional magnetic resonance imaging (MRI) performed at 3–5 days after the initial insult³. Biomarkers capable of discriminating neonates with significant brain injury, earlier in the disease course may help select candidates for synergistic neuroprotective therapies and inform clinical decision. Heart rate variability (HRV) is a non-invasive marker of autonomic functional state, known to be inversely proportional to the severity of neonatal encephalopathy⁴. It is a potential prognostic marker of neurological outcome after hypoxic-ischemic brain injury^{5,6}. The longitudinal changes in

HRV metrics during therapeutic hypothermia and its relationship with the topography of brain injury is not well understood.

HRV analysis quantifies the fluctuations in successive QRS complexes generated by heart-brain interactions and non-linear modulation of autonomic outputs. It has been suggested that high-frequency (HF) fluctuations correspond to vagal output and low-frequency (LF) fluctuations reflect baroreceptor activity during resting conditions. The respiratory cycle, either from spontaneous or assisted breathing, is imprinted in the HF component of HRV. Conversely, there is increasing evidence that it is not possible to reliably distinguish sympathetic and parasympathetic contributions to HRV⁷. The relationship between autonomic activity and spectral analysis of HRV becomes hazy at the extremes of physiology and considerable caution is needed in interpretation⁸. Traditionally, time domain and frequency domain measures of HRV in neonates with hypoxic-ischemic brain injury has been

¹Department of Paediatrics, Faculty of Health Sciences, McMaster University, Hamilton, ON, Canada. ²Department of Paediatrics, The Hospital for Sick Children, University of Toronto, Toronto, ON, Canada. ³Department of Diagnostic Imaging, The Hospital for Sick Children, University of Toronto, Toronto, ON, Canada. ⁴Bloorview Research Institute, Holland Bloorview Kids Rehabilitation Hospital, Toronto, ON, Canada. ⁵Clinical Research Unit, Children's Hospital of Eastern Ontario Research Institute, Ottawa, ON, Canada.

✉email: goswamii@mcmaster.ca

Received: 6 November 2021 Revised: 31 January 2022 Accepted: 15 February 2022

Published online: 15 March 2022

previously reported, however other HRV measures particularly Poincaré plots has not been extensively studied.

Despite methodological heterogeneity between studies, depressed HRV has been consistently reported in moderate-severe encephalopathy^{4,9–13}. Prior studies on brainstem dysfunction, coma and traumatic brain injury^{14,15} allude to direct and indirect functional links between autonomic regulation and integrity of brain structures involved in higher brain functions¹⁶. The aim of this study was to evaluate the differences in longitudinal HRV trajectory during the first 48 h of life in neonates, undergoing therapeutic hypothermia, with different patterns of hypoxic-ischemic brain injury. We hypothesized that the pattern of brain injury will influence individual neonates' early heart rate variability and how HRV changes over time.

MATERIALS AND METHODS

Participant recruitment and inclusion criteria

This was a secondary analysis of the data collected from a prospective study at The Hospital for Sick Children, Canada for neonatal encephalopathy. Encephalopathic neonates ≥ 36 weeks gestational age and recruited within 6 h of life were included in the study. For this study, we included neonates with a diagnosis of neonatal encephalopathy and who met the eligibility criteria for therapeutic hypothermia. Neonatal encephalopathy due to infectious, genetic or metabolic etiology were excluded. Decision to initiate hypothermia was ascertained based on clinical presentation, neurological examination, fetal acidosis (pH < 7 or base deficit ≥ 12), presence of peripartum sentinel event, and Apgar scores ≤ 5 at 10 min by on-call Neonatologist following therapeutic hypothermia protocol of the Neonatal intensive care unit. Research team members approached parents for consent after the decision of hypothermia was taken. A Pediatric Neurologist (ET) from the research team performed neurological examination to assign encephalopathy score within 24 h of recruitment. The institutional research ethics board approved the study protocol, and parents of all subjects provided informed consent.

Clinical assessments

All subjects underwent therapeutic hypothermia for 72 h. EEG-ECG monitoring (NicoletOne™ vEEG system, Natus, Middleton, WI) was initiated as soon as possible after admission and continued for at least 48 h after birth to capture synchronized video images with digital EEG-ECG data. Severity of encephalopathy was graded within 24 h of life using the encephalopathy scoring system, previously demonstrated to be associated with neurodevelopmental outcomes¹⁷. Severity of cardiac dysfunction was quantified within 48 h of life using the cardiovascular subscore of a previously reported multiorgan dysfunction scale i.e. score 0 (troponin T < 0.1 $\mu\text{g/L}$ and no inotropes), score 1 (troponin T 0.1–0.24 $\mu\text{g/L}$ and 1 inotrope < 24 h), score 10 (troponin T > 0.24 $\mu\text{g/L}$ and 1 inotrope > 24 h) and score 20 (> 2 inotrope)¹⁸.

ECG preprocessing and HRV computation

ECG data was sampled at 256 Hz and 1 h recordings at 12 h, 18 h, 24 h, 30 h, 36 h, 42 h and 48 h postnatal age were extracted. Our cohort included only outborn infants, thus recordings at 6 h after birth were rarely available. Time epochs with electrographic seizures in corresponding EEG recording were excluded from the analysis. Signal processing was performed using Kubios HRV analysis software, version 3.3 (Kubios Oy, Kuopio, Finland)¹⁹. A built-in QRS detection algorithm based on the Pan–Tompkins algorithm was applied to detect R-peaks and compute RR interval (Fig. 1). Cubic spline interpolation at a rate of 4 Hz generated an equidistantly sampled RR time series. An automatic artefact correction algorithm was used to detect technical and physiological artefacts and remove ectopic/misplaced beats from the normal sinus rhythm¹⁹. The detrending method based on smoothness prior to regularization with a cutoff frequency of < 0.04 Hz was used to remove non-stationarities. Frequency domain measures were estimated by Welch's periodogram method using window width of 300 s with 50% overlap and smoothing window of 0.02 Hz.

HRV metrics

Standard time domain analysis (RMSSD, Root mean square successive RR interval differences; SDNN, Standard deviation of NN interval), frequency

domain analysis (normalized LF or LFnu [0.04–0.15 Hz], normalized HF or HFnu [0.15–0.4 Hz]) and Poincaré plot (SD1,SD2) measures were calculated from each time-epoch²⁰. SDNN quantifies the overall variation or total power in the beat-to-beat interval. LFnu quantifies the percent of the total power explained by the low-frequency power. RMSSD and HFnu characterizes short-term variability or fast changes in the beat-to-beat intervals. HFnu quantifies the percent of the total power explained by the high-frequency power^{21–23}.

Poincaré analysis of consecutive RR intervals (RRi) quantifies the dispersion in the RRi in the direction perpendicular (SD1) and diagonal (SD2) to the line of identity of the scatter plot^{22,24}. The line of identity is used as a reference line in a 2-dimensional scatter plot. When the corresponding RR intervals are equal to each other (no variability), the corresponding scatter points fall exactly on the identity line (Fig. 1). SD1 denotes the deviations of the points perpendicular to the line of identity (measure of beat-to-beat variability) while SD2 denotes the dispersion of the points along the line of identity (measure of overall variability)²⁵. It has been shown experimentally that the shape of the Poincaré plot is indicative of alterations in sympathetic and parasympathetic modulation (Fig. 1)²⁵. In the presence of balanced sympathetic and parasympathetic activity, it is "comet shape". Parasympathetic blockade or unopposed sympathetic activity gives it a "cigar shape". However, complete autonomic blockade changes the shape of the plots to a "tight cluster"²⁵. We further calculated Cardiac vagal index (CVI) and Cardiac sympathetic index (CSI) from SD1 and SD2 values using the following equations:

$$\text{CVI} = \log_{10}(\text{SD1} * \text{SD2})$$

$$\text{CSI} = \text{SD2}/\text{SD1}$$

These measures are claimed to be reliable markers of short-term cardiac parasympathetic and sympathetic function separately²⁶.

Neuroimaging

MRI brain was performed using custom MR-compatible incubators with specialized head coils on a 3 T or 1.5 T MRI scanner (Siemens Magnetom Prisma or Skyra 3 T, or Philips Achieva 3 T or 1.5 T). As these images were obtained for both clinical and research purposes, sedation was used when indicated by the clinical team. Imaging sequences included T1 (TR/TE = 6/2.64, voxel size = 1 × 1 mm; slice thickness = 1 mm, field of view (FOV) = 192 mm, number of signal averages (NSA) = 1), T2 (TR/TE = 5700/144, flip angle = 120, echo train length = 19, voxel size = 1 × 1 mm; slice thickness = 1 mm, FOV = 192 mm, NSA = 1), DWI (TR/TE = 6000/108, matrix = 128 × 128, slice thickness = 3 mm, FOV = 160 mm, echo train length = 96, NSA = 3). All images were reviewed by blinded pediatric neuroradiologist (EW) to identify brain injury. Infants were stratified by outcome into two groups: (i) Normal brain MRI (ii) Abnormal brain MRI. The second group was further classified into brain injury subtypes (i) watershed-predominant pattern of injury involving the vascular watershed zones i.e. parasagittal white matter and in more severely affected infants the overlying cortex; (ii) basal ganglia-predominant pattern affecting bilaterally the central gray nuclei (ventrolateral thalami and posterior putamina) and perirolandic cortex, hippocampus and brain stem; and (iii) mixed pattern brain injury indicating injury to areas within both the above-mentioned structures²⁷.

Statistical analysis

Descriptive statistics included standard measures of central tendency and variability. We compared HRV variables between neonates with normal and abnormal brain MRI using the Mann–Whitney U test. To compare HRV metrics across brain injury subtypes and the reference group (Normal brain MRI), we fitted linear mixed effect regression models with HRV metric (dependent variable) and brain injury subtype, postnatal age, potential confounders (independent variables). The fixed effect is brain injury subtype and postnatal age while the random effect is individual subject. We used random-intercept longitudinal model with first-order autoregression covariance (AR1) structure to regress HRV metrics on a second degree polynomial time trend allowing every neonate to follow their own trajectory with a unique intercept (baseline HRV). This approach accounts for the variability in the number of data points per subject. Interaction terms between time and brain injury subtype were a-priori considered but removed from the model if they did not improve the model fit. All HRV variables were log-transformed to meet the necessary assumptions for

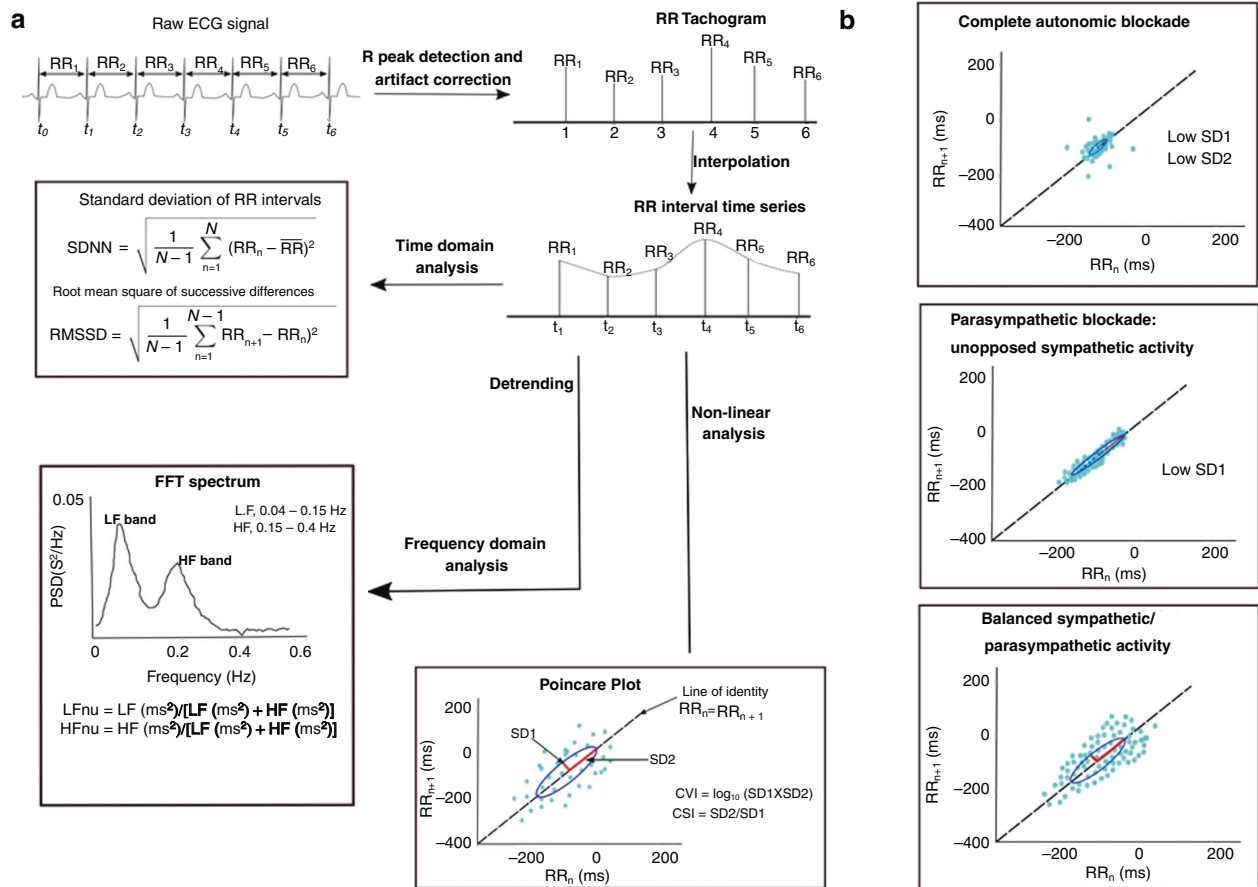


Fig. 1 The steps involved in raw ECG signal preprocessing and computation of heart rate variability metrics are illustrated. **a** Preprocessing of ECG signal includes R peak detection, artifact correction, interpolation and detrending. Subsequently, time domain (SDNN, RMSSD), frequency domain (LFnu, HFnu), and non-linear (SD1, SD2) metrics are computed. **b** Visual illustration of Poincaré plots in three different experimental situation namely complete autonomic blockade, parasympathetic blockade and balanced sympathetic-parasympathetic activity.

general linear model validity. Clinical covariates such as Apgar score at 5 min, umbilical cord arterial pH, encephalopathy scores, gestational age, sex, cardiac dysfunction score were accounted for in these models in stepwise forward method and the variables that did not improve the Akaike Information Criterion were omitted. All statistical calculations were performed using the R software package, version 3.6.2 (R Foundation for Statistical Computing, Vienna, Austria).

RESULTS

Baseline characteristics of the study participants

Among 112 infants who met the inclusion criteria, 6 infants did not have MRI brain and thus were excluded from the analyses. Further 6 infant's data had to be excluded due to poor quality of ECG signals, 3 infants did not have EEG-ECG recording, 4 infants were excluded because continuous EEG-ECG monitoring was started after 36 h of life and 4 infants were excluded from the study due to later diagnosis of other pathologies. Among 89 infants who were included in the final analysis, specific time-epochs with corresponding electrographic seizures were excluded. Since the study was conducted in an outborn center, due to delay in initiation of EEG-ECG recording the data at early time points (6 h) was often not feasible. ECG data available from 31 epochs (12 h), 53 epochs (18 h), 78 epochs (24 h), 81 epochs (30 h), 87 epochs (36 h), 87 epochs (42 h) and 86 epochs (48 h) infants were included in the analyses. Table 1 enumerates the demographic characteristics of the study participants. Five subjects died prior to discharge. Among the infants who had abnormal brain MRI brain ($n = 40$), 15 (38%) had focal infarcts,

8 (20%) had basal ganglia-predominant pattern, 5(13%) had watershed-predominant pattern, and 12 (30%) had mixed pattern of injury. Neonates with abnormal brain MRI had significantly higher first blood lactate level, higher needs for ionotrope infusion and anti-epileptic medication and higher incidence of both electroclinical and subclinical electrographic seizures than neonates with normal brain MRI. There was no clinically significant difference between the median encephalopathy score of neonates with and without abnormal brain MRI in the first 24 h of birth.

Comparison of HRV metrics at specific timepoints between brain injury groups

There was no statistically significant difference between the mean HRV values of neonates with normal brain MRI and abnormal brain MRI at 12 h of life. Neonates with abnormal brain MRI had significantly lower mean SDNN and SD2 values at all timepoints beyond 18 h of life and significantly lower RMSSD and SD1 values at 18 h, 24 h, 30 h and 36 h of life compared to neonates with normal brain MRI. The mean difference in LFnu and HFnu values between the two groups was only statistically significant at 24 h, 30 h and 36 h of life (Table 2). Beyond 24 h of life, there was a statistically significant difference in CVI and CSI values between the two groups, with lower values in neonates with abnormal brain MRI.

Comparison of the HRV metrics between different brain injury subtypes

Figure 2 shows the mean HRV values (± 1 SEM) as a function of postnatal age and brain injury subtype. The mean HRV values were comparable between neonates with normal brain MRI and

Table 1. Perinatal and neonatal characteristics of the study participants.

	Entire Cohort	Normal MRI	Abnormal MRI	<i>p</i> value
<i>N</i>	89	49	40	
Male, <i>n</i> (%)	56 (62)	31 (63.2)	25(62.5)	0.94
Gestational age, mean (SD)	39.5 ± 1.3	39.6 ± 1.4	39.3 ± 1.2	0.33
Birth weight, mean (SD)	3342 ± 511	3393 ± 520	3277 ± 501	0.29
C-section, <i>n</i> (%)	51 (57)	23 (46.9)	28(70)	0.03
Apgar score at 1 min, median (IQR)	1 (1–3)	1 (1–3)	1(1–3)	0.72
Apgar score at 5 min, median (IQR)	4 (3–6)	5 (3–6)	4 (3–6)	0.59
Arterial cord pH, mean (SD)	7.09 ± 0.17	6.98 ± 0.14	7.00 ± 0.18	0.61
First gas lactate, mean (SD)	9.9 ± 6.1	7.8 ± 4.9	12.73 ± 6.2	<0.0001
Time to reach target temperature (hr), mean (SD)	4.4 ± 1.6	4.3 ± 1.8	4.5 ± 1.8	0.61
AED, <i>n</i> (%)	47 (52)	17 (34.6)	30(75)	0.0002
Electroclinical seizures, <i>n</i> (%)	16 (18)	5 (10.2)	11(27.5)	0.03
Clinical seizures, <i>n</i> (%)	29 (32)	13 (26.5)	16(40)	0.17
Electrographic seizures only, <i>n</i> (%)	18 (20)	2 (4)	16(40)	<0.0001
Encephalopathy score, median (IQR)	5 (4–6)	4 (3–5)	5 (4–6)	0.002
Inotrope infusion, <i>n</i> (%)	32 (35)	13 (26)	19(48)	0.02
Cardiovascular dysfunction score ≥ 10 <i>n</i> (%)	13(14.6)	6(12)	7(17.5)	0.58

AED Anti-epileptic drugs, SD standard deviation, IQR Interquartile range.

Chi-square/Fischer exact test (categorical data) Student *t* test (continuous/ordinal data).

Abnormal MRI includes: Watershed-predominant pattern, Basal ganglia-predominant pattern, Mixed pattern of brain injury and focal injury.

focal infarcts at all time points. At baseline (12 h) HRV measures were suppressed in infants with basal ganglia pattern [LFnu 80.1 ± 4.8 (*p* = 0.99), SDNN 9.7 ± 3.6 msec (*p* = 0.69), RMSSD 7.02 ± 2.7 msec (*p* = 0.71), SD1 4.9 ± 1.9 msec (*p* = 0.68), SD2 12.8 ± 4.9 msec (*p* = 0.81), CVI 1.6 ± 0.4 (*p* = 0.85), CSI 2.8 ± 0.2 (*p* = 0.99)] and infants with mixed pattern [LFnu 57.1 ± 11.9 (*p* = 0.19), SDNN 3.4 ± 1.4 msec (*p* = 0.02), RMSSD 4.2 ± 1.3 msec (*p* = 0.07), SD1 2.9 ± 0.9 msec (*p* = 0.07), SD2 3.9 ± 1.9 msec (*p* = 0.01), CVI 0.8 ± 0.3 (*p* = 0.03), CSI 1.1 ± 0.2 (*p* = 0.005)] but similar in infants with focal infarcts [LFnu 74.2 ± 13.4 (*p* = 0.09), SDNN 27.2 ± 5.9 msec (*p* = 0.77), RMSSD 24.8 ± 5.7 msec (*p* = 0.36), SD1 17.5 ± 4.1 msec (*p* = 0.36), SD2 34 ± 7.4 msec (*p* = 0.86), CVI 2.5 ± 0.3 (*p* = 0.51), CSI 2.1 ± 0.2 (*p* = 0.99)] compared to infants with normal brain MRI [LFnu 78.4 ± 2.5, SDNN 16.7 ± 2.2 msec, RMSSD 12.9 ± 1.7 msec, SD1 9.13 ± 1.2 msec, SD2 21.7 ± 3.03 msec, CVI 2.1 ± 0.2, CSI 2.4 ± 0.2]. Compared to infants with Normal MRI had significantly higher HFnu [21.5 ± 2.5] than infants with mixed pattern injury [HFnu 42.1 ± 11.5 (*p* = 0.2)]. Moreover, neonates with mixed pattern injury had significantly lower mean SD2, SDNN, CSI and CVI values at all timepoints in the first 48 h of life than infants with Normal MRI (Fig. 2). Mixed pattern injury group also had significantly lower LFnu and higher HFnu compared to Normal MRI group beyond 30 h of life. Infants with basal-ganglia predominant injury had lower SDNN, RMSSD, SD1, SD2 values than infants with Normal MRI especially in the first 12–30 h of life, but the difference was not statistically significant.

Association of brain injury subtype and HRV trajectory adjusted for clinical covariates

The goal of mixed effect modeling was to determine the effect of brain injury subtype on individual HRV metric while adjusting for postnatal age and relevant clinical covariates. The clinical covariates that significantly improved the model were encephalopathy score at 0–24 h postnatal age, cardiovascular dysfunction score at 0–48 h postnatal age, and exposure to anti-epileptic drugs. After accounting for these clinical covariates, there was a significant effect of brain injury subtype on individual HRV metrics. Posthoc analyses indicated that at any given timepoint neonates

with mixed pattern of brain injury exhibited lower SDNN ($\beta = -0.38$, $p < 0.001$), RMSSD ($\beta = -0.25$, $p = 0.02$), LFnu ($\beta = -0.13$, $p < 0.001$), CVI ($\beta = -0.67$, $p < 0.001$), CSI ($\beta = -0.77$, $p = 0.003$) and higher HFnu ($\beta = 0.26$, $p = 0.001$) compared to neonates with normal brain MRI. Similarly, neonates with watershed predominant pattern of injury exhibited significantly lower SDNN ($\beta = -0.78$, $p = 0.08$), RMSSD ($\beta = -0.63$, $p = 0.04$), LFnu ($\beta = -0.16$, $p = 0.11$), CVI ($\beta = -1.42$, $p = 0.009$), CSI ($\beta = -0.91$, $p = 0.23$) and higher HFnu ($\beta = 0.34$, $p = 0.14$) compared to neonates with normal brain MRI (Table 3, Supplementary Table 1). The model did not improve with addition of interaction term for brain injury subtype with postnatal age and thus was omitted from the final model. Lack of significant interaction with postnatal age indicates that the pattern of change in each HRV metric over the first 48 h of life was similar in all brain injury subtype. There was noted to be transient decrease in SDNN, RMSSD, SD1, SD2, CVI in the first 30 h followed by a subsequent increase upto 48 h (Supplementary Table 1, Supplementary Fig. 1). On the contrary, the frequency domain measures (LFnu, HFnu) and CSI remained unchanged over time.

Visual interpretation of Poincaré maps

Cardiac dynamics can be visually compared by the topography of Poincaré maps between infants with different brain injury subtypes. Figure 3 demonstrates Poincaré maps derived from a single time-epoch of four patients with different brain injury patterns. Mixed pattern of brain injury was characterized by both low SD1 and SD2 represented by a “tight cluster”. Basal ganglia pattern was found to have low SD1 depicted as a “cigar-shaped” pattern. Infants with normal brain MRI or focal injury were noted to have high SD1 and SD2 generating a “comet-shaped” pattern.

DISCUSSION

The current study illustrates an association between the degree of autonomic impairment during hypothermia therapy and the pattern of hypoxic-ischemic brain injury on MRI. Early treatment decisions in neonatal encephalopathy after perinatal hypoxic-

Table 2. Comparison of HRV metrics at specific timepoints between normal and abnormal MRI groups.

Age of life (hours)	HRV Metrics	Normal MRI	Abnormal MRI	p value
12	No. of subjects	15	16	
	SDNN (ms)	15 (11–23)	9.1 (2.7–24.2)	0.31
	RMSSD (ms)	11.2 (8.9–18.5)	7.7 (3.5–25.3)	0.55
	SD1	7.9 (6.3–13)	5.5 (2.5–17.9)	0.55
	SD2	19.8 (14.2–28.9)	11.7 (3.5–29)	0.28
	CVI	2.1 (2–2.55)	1.8 (0.9–2.7)	0.44
	CSI	2.3(2–3.1)	2 (1.4–2.6)	0.14
	LFnu	79 (72–85)	71.3 (63–83)	0.28
	HFnu	20.1 (15.2–27.3)	28.5 (16.3–36.4)	0.29
18	No. of subjects	29	24	
	SDNN (ms)	14 (7.5–17.3)	4.8 (2.7–14.8)	0.01
	RMSSD (ms)	9.2 (4.9–18)	4.2 (3–8)	0.01
	SD1	6.5 (3.4–12.9)	3 (2.1–5.7)	0.01
	SD2	18.8 (10.1–23)	6.1 (2.8–19.4)	0.01
	CVI	2.1 (1.5–2.3)	1.25 (0.9–2.1)	0.009
	CSI	2.5 (1.6–3)	1.7 (1.3–2.4)	0.09
	LFnu	82.4 (68.1–86)	80.1 (68–83)	0.55
	HFnu	17.5 (14–31.8)	19.8 (16.7–31.7)	0.55
24	No. of subjects	45	33	
	SDNN (ms)	12 (6.9–19.1)	4.4 (2.3–9.2)	0.002
	RMSSD (ms)	9.1 (4.3–11.5)	4 (2.9–7.4)	0.004
	SD1	6.5 (3–8.1)	2.8 (2.1–5.3)	0.004
	SD2	15 (9.3–25.2)	4.6 (2.2–12.7)	0.002
	CVI	2.0 (1.5–2.3)	1.2 (0.7–1.6)	0.002
	CSI	2.4 (1.8–3.1)	1.8 (1.2–2.3)	0.03
	LFnu	82.7 (69–87)	74.8 (60.3–87.5)	0.25
	HFnu	17.2 (12–30.1)	25.1 (12.5–39.5)	0.26
30	No. of subjects	46	35	
	SDNN (ms)	10 (6–16)	4.8 (2.8–10.6)	0.002
	RMSSD (ms)	6.5 (4.3–11.8)	4.5 (3.2–7.4)	0.02
	SD1	4.6 (3.2–8.4)	3.2 (2.3–5.3)	0.02
	SD2	13.6 (7.9–21.4)	5.7 (2.5–14.1)	0.001
	CVI	1.7 (1.4–2.3)	1.2 (0.9–1.8)	0.004
	CSI	2.4 (2–3.2)	1.6 (1–2.7)	0.001
	LFnu	82.1 (73–89)	76 (52–85)	0.04
	HFnu	17.7 (10–26)	23.1 (14.1–47.1)	0.04
36	No. of subjects	49	38	
	SDNN (ms)	10.2 (6.2–13.7)	5.9(1.9–11.5)	0.007
	RMSSD (ms)	7 (4.8–10.6)	4.4 (2.7–9.6)	0.05
	SD1	5.0 (3.4–7.5)	3.1 (1.9–6.8)	0.05
	SD2	13.2 (7.8–16.6)	6.2 (1.9–14.4)	0.003
	CVI	1.8 (1.4–2.1)	1.4 (0.6–2)	0.01
	CSI	2.5 (1.9–3)	1.6 (1.2–2.4)	<0.001
	LFnu	83 (74–87)	75 (58–81)	0.006
	HFnu	17 (13–25)	25 (18–41)	0.007
42	No. of subjects	49	38	
	SDNN (ms)	11.6 (7.1–18.7)	7.8 (4–14.5)	0.02
	RMSSD (ms)	8 (5.2–15.5)	5.7 (3.9–11.7)	0.11
	SD1	5.7 (3.7–10.9)	4.1 (2.7–8.3)	0.11
	SD2	15 (9.4–24.2)	10.3 (3.9–18.1)	0.02
	CVI	1.9 (1.5–2.4)	1.6 (1.2–2.2)	0.03

Table 2. continued

Age of life	HRV Metrics	Normal MRI	Abnormal MRI	p value
	CSI	2.3 (1.8–2.9)	1.8 (1.2–2.5)	0.009
	LFnu	80.1 (73–88)	79 (61–83)	0.09
	HFnu	19.8 (11.5–26.8)	20.9 (16.2–38.1)	0.09
48	No. of subjects	48	38	
	SDNN (ms)	12.8 (7.6–22.1)	6.4 (4.9–14.6)	0.006
	RMSSD (ms)	9.5 (6–18)	6.9 (3.8–15.6)	0.07
	SD1	6.7 (4.2–12.8)	4.9 (2.7–11.1)	0.07
	SD2	16.8 (10.1–29.4)	7.8 (5.3–18.8)	0.003
	CVI	2.0 (1.7–2.6)	1.6 (1.1–2.3)	0.009
	CSI	2.3 (1.9–2.8)	1.9 (1.2–2.5)	0.007
	LFnu	81.7 (74–86)	75.8 (60.5–85.3)	0.11
	HFnu	18.2 (13–25.7)	24.1 (14.5–38.9)	0.11

Median (Interquartile range). Mann–Whitney U test.

SDNN Standard deviation of RR intervals, RMSSD Root-mean-square difference between adjacent RR intervals, LF Low frequency, HF High frequency. Abnormal MRI includes: Watershed-predominant pattern, Basal ganglia-predominant pattern, Mixed pattern of brain injury and focal injury.

ischemic insult are primarily based on the knowledge of clinical outcomes and their association with severity of the encephalopathy. A biomarker that facilitates prognostication before and during hypothermia therapy would help tailor neuroprotective therapies according to an individual's biological profile and treatment response. This exploratory study demonstrates the promise of characterizing disease heterogeneity by providing some insight into the autonomic functional state. It is well known that basal ganglia and thalamic injury predicts poor neuromotor outcomes, while cortical watershed-type injuries relate to school-aged cognitive deficits and learning disabilities²⁸. However, MRI after completion of hypothermia is a static indication of the response to hypothermia therapy in an isolated timeframe. Our results suggest assessment of HRV in neonates undergoing hypothermia may help differentiate the subcohort that may have watershed or mixed pattern of brain injury from minor brain injuries earlier than routine clinical MRI.

A differential autonomic response was noted between the group of neonates who progressed to abnormal brain MRI compared to neonates with normal brain MRI beyond 18 h of life. The neonates with an abnormal brain MRI showed significantly lower overall variability (SDNN, SD2) and beat-to-beat variance (RMSSD, SD1). Furthermore, neonates with abnormal brain MRI had lower LF fluctuations and higher HF fluctuations between 30–36 h of life. The negative correlation between HRV measures and severity of brain injury is consistent with previous studies^{9–13}. Whether assessed at one week of life⁹ or at any point within the first 72 h^{29,30}, lower LF/HF ratio has been consistently associated with severe encephalopathy and adverse neurodevelopmental outcomes. Compared to previous studies which assessed HRV sampling at single timepoints, our study quantifies autonomic dysfunction at multiple timepoints longitudinally in the context of the evolving process of brain injury. Although the neonates with abnormal brain MRI were clinically more sick and likely to have seizures than neonates with normal brain MRI, none of the HRV measures were significantly different at 12 h of life between the two groups. This finding suggests that single time point assessment of especially in the first 12h–18h of life may be unable to differentiate neonates with abnormal brain MRI from normal brain MRI.

Within the group of neonates with abnormal brain MRI, the most severe dampening of HRV measures was observed with watershed predominant pattern and mixed pattern of injury even after adjustment for severity of encephalopathy, cardiac dysfunction and exposure to anti-seizure medications, suggesting

that substantial white matter injury may independently contribute to autonomic impairment. Neonates with basal ganglia predominant pattern were characterized by higher HRV measures than mixed/watershed predominant injury but lower than the neonates with normal brain MRI or focal injury. Contrary to our findings, Metzler et al. found that neonates with watershed predominant pattern in their study had less severe HRV suppression than predominant basal-ganglia injury/global injury¹². This difference may be explained by the differences in classification of neonates into brain injury groups between the two studies. We considered predominant deep gray matter injury and mixed pattern injury as separate groups while Metzler et al. classified them deep gray injury with global injury neonates in the same group while considering death as a separate group. Studies using fMRI in humans and animal studies has reported that the critical sites in the cerebral cortex may be involved in autonomic control³¹. Complex interconnections within the central autonomic network, which includes the insular cortex, anterior cingulate cortex, prefrontal cortex, amygdala, hypothalamus, and corresponding projections to the brain stem influencing vagal and sympathetic preganglionic neurons drives cardiovascular modulation³². This network is well developed at term gestation with evidence of lateralization in central autonomic control^{33,34}. Right insular cortex injury is believed to result in decreased activity in the right sympathetic chain, same baroreceptor sensitivity but lower operating blood pressure, prolonged QT interval, decreased HRV or contralateral unbalanced parasympathetic overactivity with risk of bradyarrhythmia and asystole. On the otherhand, left insular cortex injury results in decreased parasympathetic output from the brain, decreased activity in the left sympathetic chain, decreased baroreceptor sensitivity, decreased cardiac function and contralateral unbalanced sympathetic overactivity³⁵. It is likely that acute hypoxic injury to the parasagittal white matter and subcortical structures might compromise these functional connections indicating a possible mechanistic link.

Frequency domain HRV measures in relation to hypoxic-ischemic brain injury have been extensively studied^{4,9–11,13}. Interestingly, this study demonstrates that at early time points 12–24 h, the dampening of time domain measures (SDNN/RMSSD) and SD1, SD2 in neonates with significant brain injury was statistically significant rather than the frequency domain measures (LFnu, HFnu). Previously, Goulding et al. reported that HRV features were most predictive of a normal outcome at 24 h (SDNN, LF) and abnormal neurological outcome at 48 h (SDNN, HF)¹⁰. The best predictive performance of LF and HF power in

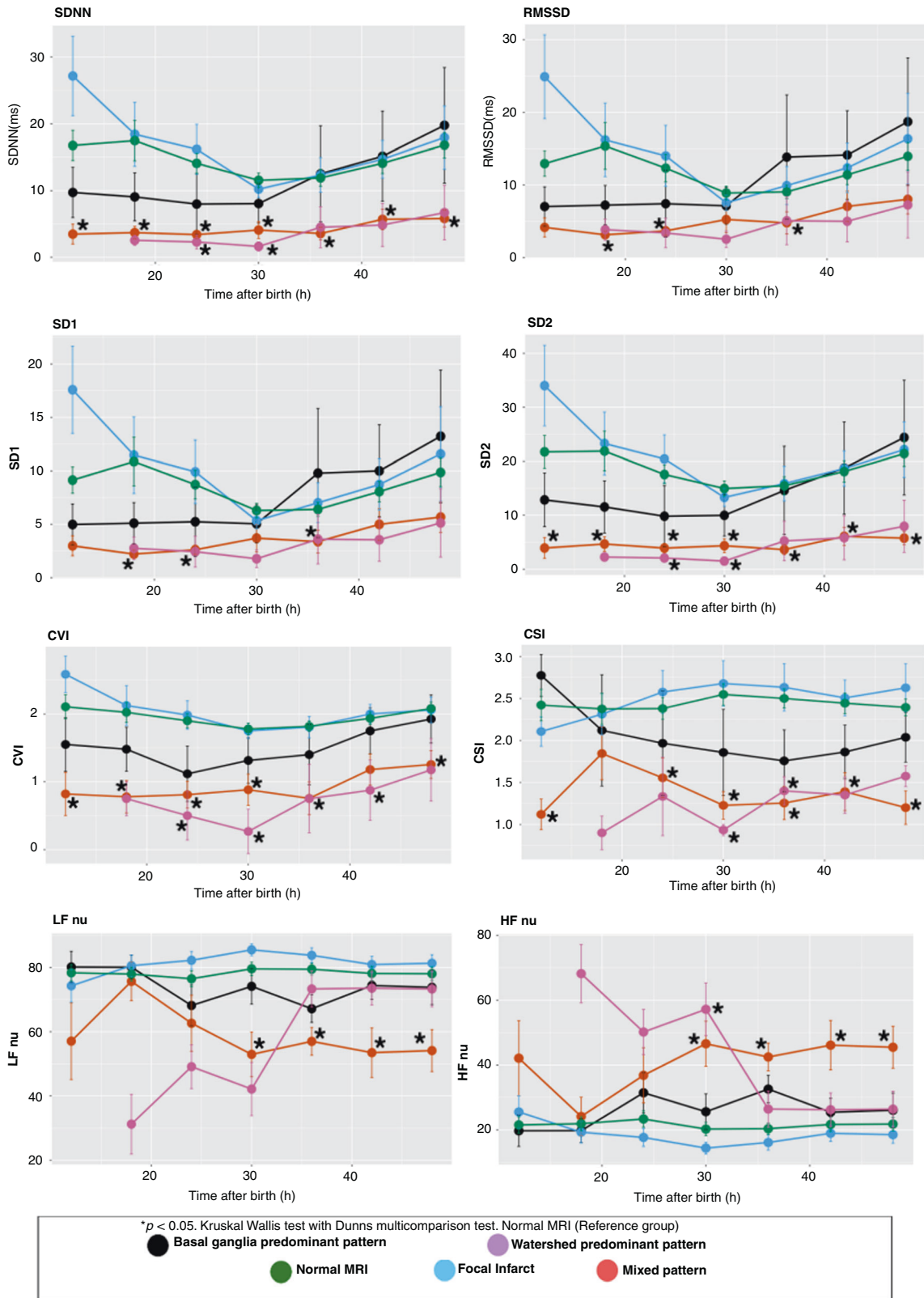


Fig. 2 Mean (SEM) of common HRV metrics in the first 48 h of life in infants with different subtypes of brain injury (color coded). Watershed and Mixed pattern of injury was associated with most severely depressed while basal ganglia injury was associated with moderately depressed short-term (RMSSD, SD1) and overall variability (SDNN, SD2) at all timepoints compared to infants with normal MRI or focal infarct. There were no significant differences in the temporal trends of frequency domain HRV measures between the groups.

Table 3. Summary of the multivariable mixed effects model showing the effect of the pattern of brain injury on mean HRV metrics on average over the first 48 h.

	Watershed predominant	Basal ganglia predominant	Mixed Pattern	Focal Injury
	(HRV measure in brain injury type/HRV measure in Normal MRI) at any given postnatal age			
SDNN	0.63 (0.45–0.88)*	0.86 (0.69–1.08)	0.64 (0.52–0.80)**	1.01 (0.86–1.19)
RMSSD	0.74 (0.52–1.04)	0.93 (0.74–1.17)	0.75 (0.60–0.93)*	1.01 (0.85–1.19)
LFnu	0.89 (0.80–1.00)*	0.97 (0.91–1.04)	0.85 (0.80–0.91)**	1.03 (0.97–1.08)
HFnu	1.32 (0.81–1.72)*	1.15 (0.97–1.36)	1.32 (1.12–1.55)**	0.93 (0.82–1.06)
SD1	0.74 (0.55–1.00)	0.94 (0.76–1.17)	0.76 (0.61–0.93)*	1.01 (0.86–1.19)
SD2	0.59 (0.42–0.83)*	0.83 (0.67–1.06)	0.59 (0.48–0.75)**	1.02 (0.86–1.21)
CVI	0.44 (0.22–0.85)*	0.78 (0.50–1.23)	0.45 (0.29–0.69)**	1.03 (0.73–1.44)
CSI	0.43 (0.19–0.94)*	0.65 (0.38–1.1)	0.44 (0.27–0.71)*	1.06 (0.71–1.58)

The effect on each metric is expressed as the ratio of the mean value for the particular brain injury pattern over the normal MRI, calculated by exponentiating the beta coefficient estimate from the fitted model. 95% Confidence Intervals are also shown. Values less than 1 indicate suppression of variability metric and value larger than 1 indicates increased in variability metric.

p* value < 0.05, *p* value < 0.001.

Adjusted for cardiac dysfunction score, encephalopathy score at 24 h, exposure to anti-epileptic drugs.

Normal brain MRI as reference.

differentiating normal from abnormal neurodevelopmental outcomes is around 24 h¹¹. Using SD1,SD2 or derived measures (CVI, CSI) may have some technical advantages over frequency domain and time domain measures. Firstly, mild changes in the short-term cardiac sympathetic (CSI) and parasympathetic (CVI) function can be assessed simultaneously and separately. Secondly, smaller epochs (<2 min) are sufficient for calculation of SD1 and SD2. The strong correlation between SD1-RMSSD pair and SD2-SDNN pair seen in our study further suggests that SD1/SD2 can be used as an alternative to time domain metrics. Time domain metrics are preferably measured over 24 h time epochs of ECG recordings and require standardization of time-epoch lengths to ensure comparability between patients. Lastly changes can be interpreted visually at bedside by Poincaré plots, which provides both summary and detailed beat-to-beat information. Superiority of Poincaré plots in yielding more reliable indices compared to frequency domain measures have been previously documented²⁶. This raises the exciting possibility of using short-term moving window Poincaré plot to develop ECG-based monitoring tool for longitudinal bedside assessment of autonomic functional state.

Prior studies have suggested that abnormal neurodevelopmental outcome after hypoxic-ischemic brain injury is associated with increased parasympathetic and decreased sympathetic activity^{9,11}. This has been attributed to (i) a protective role of preserved sympathetic activity following hypoxic injury in maintaining adequate systemic blood pressure and cerebral perfusion; or (ii) more extensive subcortical brain injury might inhibit sympathetic activity. Our results indicate that significant white matter injury was associated with both suppressed CVI and CSI suggestive of global suppression of both arms of the autonomic system rather than the typical theoretical expectations of "increased parasympathetic activity". Goulding et al. also found that severe encephalopathy had both reduced HF and LF power, implying a reduction in overall autonomic function¹⁰. This study highlights the need for a shift in the understanding of autonomic responses following hypoxic-ischemic brain insult, because a simple reciprocal relationship between the sympathetic and parasympathetic activity may not hold true in this cohort. Global autonomic suppression may signify poor responsiveness to regulatory mechanisms and decreased adaptability to stress.

An ideal real-time monitoring modality must be capable of identifying critical phases in the disease evolution and response to intervention. Our data demonstrates a trend towards transient decrease in time domain HRV measures followed by subsequent increase with a nadir at 30 h, suggesting that these measures may

be potential markers to follow disease evolution. This pattern is consistent across all infants irrespective of the brain injury subtype. The initial decrease in HRV may correspond to early incremental cerebral edema and increasing intracranial pressure³⁶. A subsequent increase in HRV may reflect recovery of cerebral function possibly related to the neuroprotective effects of hypothermia. These findings reiterates Massaro et al's previous suggestion that profound reduction in HRV around 24 h may indicate failure of hypothermia therapy to prevent secondary brain injury¹¹. Clinical validity of using longitudinal changes in HRV measures in the context of evolving brain injury will need to be further explored.

The strengths of this study includes generalizability due to a pragmatic approach taken to identify study cohort using uniform hypothermia protocol. This study was limited by the lack of a control group. Normative standards of HRV values in the first 24 h of life for healthy term infants have been recently published³⁷. The mean HRV measures in neonates with normal brain MRI or focal injury were similar and only slightly lower than the normative standards, which might be ascribed to the effect of hypothermia known to suppress HRV³⁶. Therefore, neonates who have HRV preserved during hypothermia are most likely to have minimal residual brain injury. Absence of data prior to 12 h and small sample size at 12 h restricts our ability to make robust inferences at early timepoint. The study was conducted in a outborn center and all subjects were transferred to the tertiary care unit prior to initiation of monitoring. While seizure is known to have a complex interaction with HRV³⁷, the true effect on various HRV parameters are unknown. We excluded time epochs that had electrographic seizures in the simultaneously recorded EEG signals and multivariate models were adjusted for exposure to antiseizure medication. However, it is not enough to control for administration of anti-seizure medications, which typically have long half-lives and drug levels were not measured. We also acknowledge that the sample size was limited in the watershed group, and thus caution is warranted in the comparison of watershed injury to other brain injury subtypes, which had a higher N. Lastly, we have not accounted for respiratory oscillations from spontaneously breathing versus mechanical ventilation rate on RRi analysis³⁸. Further studies intending to validate the use of Poincaré analysis at the bedside will need to account for the oscillations originating from the ventilator-assisted breathing. We also acknowledge that a small proportion of neonates in this cohort (16%) were scanned on 1.5T (rest 3T). The reasons for doing so were random such as need for scanning on weekend and not related to the acuity of the

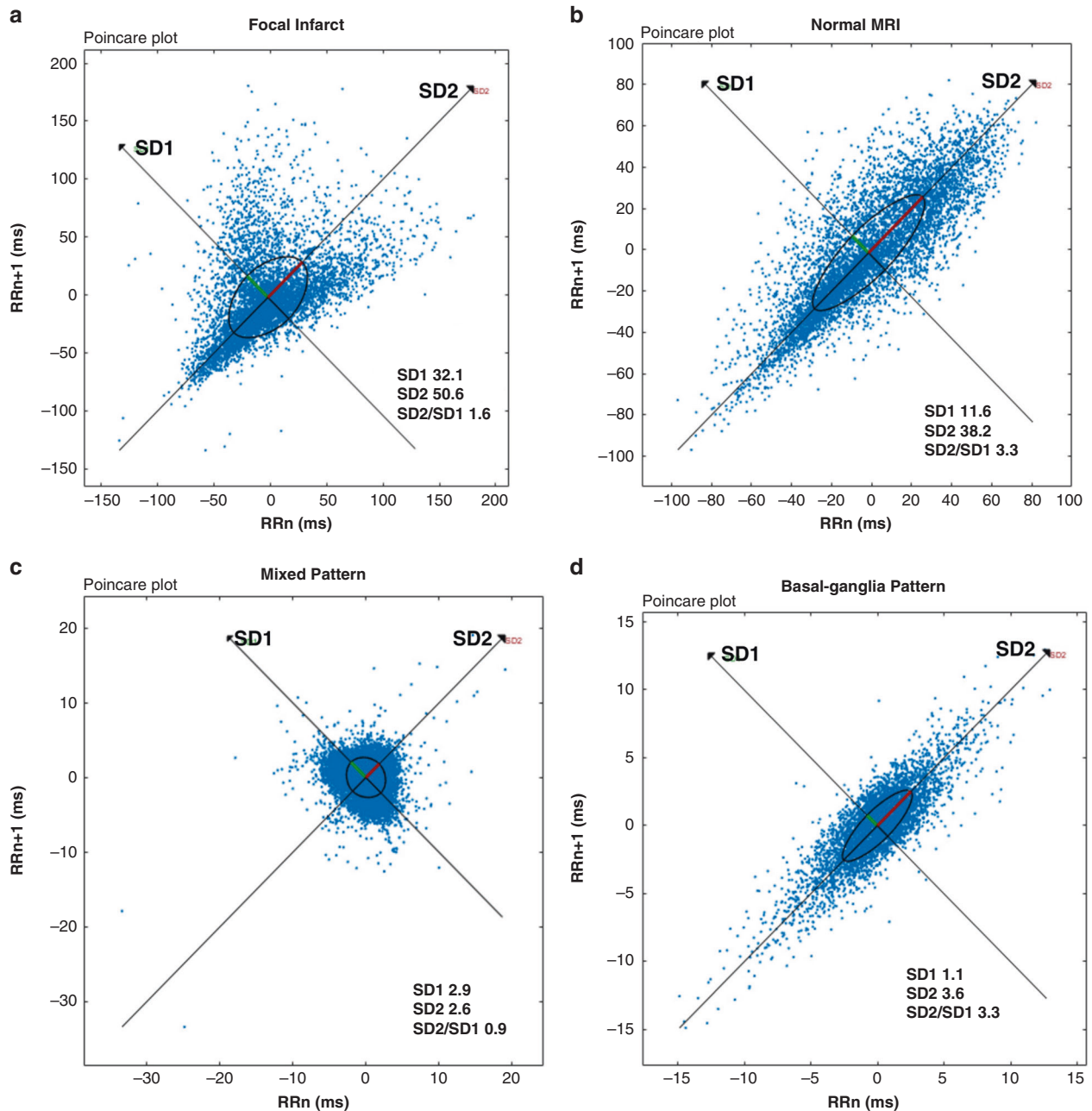


Fig. 3 Comparing the topography of Poincare maps at 12 h of life. Each plot from one patient of each brain injury subtype **a** Focal infarct, comet shaped; **b** basal ganglia pattern, cigar shaped; **c** mixed pattern of brain injury, tight cluster; **d** normal brain MRI, comet shaped.

infant's medical condition. This difference is unlikely to affect the overall qualitative Barkovich scoring reported in this manuscript³⁹. 3T has higher signal-to-noise ratio than 1.5T and even the mean differences in quantitative measures are small (mean difference in MD estimated at 1.2%)⁴⁰. Hence, the difference in magnetic field strength of the scanner was unlikely to have a substantial impact or bias on the study findings.

HRV monitoring during hypothermia provides early insights into the brain injury patterns in neonates undergoing therapeutic hypothermia. HRV metrics may potentially serve to identify neonates in need for adjuvant neuroprotective therapies. Neonates who progressed to have significant brain injury involving both watershed regions with or without deep gray matter injury demonstrated global autonomic dysfunction. Collectively, these data provides the preliminary foundation to explore the use of HRV metrics to optimize risk stratification and treatment. Our findings

provides impetus for future research to better understand the role of dysautonomia in the pathogenesis of secondary brain injury.

REFERENCES

- Jacobs, S. E. et al. Cooling for newborns with hypoxic ischaemic encephalopathy. *Cochrane Database Syst. Rev.* Cd003311 (2013).
- Tagin, M. A., Woolcott, C. G., Vincer, M. J., Whyte, R. K. & Stinson, D. A. Hypothermia for neonatal hypoxic ischemic encephalopathy: an updated systematic review and meta-analysis. *Arch. Pediatr. Adolesc. Med.* **166**, 558–566 (2012).
- Miller, S. P. et al. Patterns of brain injury in term neonatal encephalopathy. *J. Pediatr.* **146**, 453–460 (2005).
- Goulding, R. M. et al. Heart rate variability in hypoxic ischemic encephalopathy during therapeutic hypothermia. *Pediatr. Res.* **81**, 609–615 (2017).
- Andersen, M., Andelius, T. C. K., Pedersen, M. V., Kyng, K. J. & Henriksen, T. B. Severity of hypoxic ischemic encephalopathy and heart rate variability in neonates: a systematic review. *BMC Pediatr.* **19**, 242 (2019).

6. Oliveira, V. et al. Prognostic accuracy of heart rate variability analysis in neonatal encephalopathy: a systematic review. *Neonatology* **115**, 59–67 (2019).
7. Shaffer, F. & Ginsberg, J. P. An overview of heart rate variability metrics and norms. *Front. Public Health* **5**, 258–258 (2017).
8. Malik, M. & Camm, A. J. Components of heart rate variability—what they really mean and what we really measure. *Am. J. Cardiol.* **72**, 821–822 (1993).
9. Aliefendioglu, D., Dogru, T., Albayrak, M., Dibekmisirlioglu, E. & Sanli, C. Heart rate variability in neonates with hypoxic ischemic encephalopathy. *Indian J. Pediatr.* **79**, 1468–1472 (2012).
10. Goulding, R. M. et al. Heart rate variability in hypoxic ischemic encephalopathy: correlation with Eeg grade and 2-Y neurodevelopmental outcome. *Pediatr. Res* **77**, 681–687 (2015).
11. Massaro, A. N. et al. Heart rate variability in encephalopathic newborns during and after therapeutic hypothermia. *J. Perinatol.* **34**, 836–841 (2014).
12. Metzler, M. et al. Pattern of brain injury and depressed heart rate variability in newborns with hypoxic ischemic encephalopathy. *Pediatr. Res* **82**, 438–443 (2017).
13. Vergales, B. D. et al. Depressed heart rate variability is associated with abnormal EEG, MRI, and death in neonates with hypoxic ischemic encephalopathy. *Am. J. Perinatol.* **31**, 855–862 (2014).
14. Baguley, I. J., Nott, M. T., Slewa-Younan, S., Heriseanu, R. E. & Perkes, I. E. Diagnosing dysautonomia after acute traumatic brain injury: evidence for over-responsiveness to afferent stimuli. *Arch. Phys. Med Rehabil.* **90**, 580–586 (2009).
15. Estévez-Báez, M. et al. Autonomic impairment of patients in coma with different Glasgow coma score assessed with heart rate variability. *Brain Inj.* **33**, 496–516 (2019).
16. Riganello, F., Garbarino, S. & Sannita, W. G. Heart rate variability, homeostasis, and brain function. *J. Psychophysiol.* **26**, 178–203 (2012).
17. Miller, S. P. et al. Clinical signs predict 30-month neurodevelopmental outcome after neonatal encephalopathy. *Am. J. Obstet. Gynecol.* **190**, 93–99 (2004).
18. Alsina, M. et al. The severity of hypoxic-ischemic encephalopathy correlates with multiple organ dysfunction in the hypothermia era. *Pediatr. Crit. Care Med* **18**, 234–240 (2017).
19. Tarvainen, M., Niskanen, J.-P., Lipponen, J., Ranta-Aho, P. & Karjalainen, P. Kubios Hrv – heart rate variability analysis software. *Comput. Methods Prog. Biomed.* **113**, 210–220 (2013).
20. Heart Rate Variability: Standards of Measurement. Physiological interpretation and clinical use. Task Force of the European Society of Cardiology and the North American Society of Pacing and Electrophysiology. *Circulation* **93**, 1043–1065 (1996).
21. Ernst, G. Hidden signals—the history and methods of heart rate variability. *Front. Public Health* **5**, 265 (2017).
22. Shaffer, F. & Ginsberg, J. P. An overview of heart rate variability metrics and norms. *Front Public Health* **5**, 258 (2017).
23. Thomas, B. L., Claassen, N., Becker, P. & Viljoen, M. Validity of commonly used heart rate variability markers of autonomic nervous system function. *Neuro-psychobiology* **78**, 14–26 (2019).
24. Sassi, R. et al. Advances in heart rate variability signal analysis: joint position statement by the E-Cardiology Esc Working Group and the European Heart Rhythm Association Co-Endorsed by the Asia Pacific Heart Rhythm Society. *Europace* **17**, 1341–1353 (2015).
25. Brennan, M., Palaniswami, M. & Kamen, P. Poicare plot interpretation using a physiological model of Hrv based on a network of oscillators. *Am. J. Physiol. Heart Circulatory Physiol.* **283**, H1873–H1886 (2002).
26. Toichi, M., Sugiura, T., Murai, T. & Sengoku, A. A new method of assessing cardiac autonomic function and its comparison with spectral analysis and coefficient of variation of R-R interval. *J. Auton. Nerv. Syst.* **62**, 79–84 (1997).
27. Chau, V., Poskitt, K. J., Dunham, C. P., Henderson, G. & Miller, S. P. Magnetic resonance imaging in the encephalopathic term newborn. *Curr. Pediatr. Rev.* **10**, 28–36 (2014).
28. Miller, S. P. et al. Patterns of brain injury in term neonatal encephalopathy. *J. Pediatrics* **146**, 453–460 (2005).
29. Matic, V. et al. Heart rate variability in newborns with hypoxic brain injury. *Adv. Exp. Med. Biol.* **789**, 43–48 (2013).
30. Yasova Barbeau, D. et al. Heart rate variability and inflammatory markers in neonates with hypoxic-ischemic encephalopathy. *Physiol. Rep.* **7**, e14110 (2019).
31. Cechetto, D. F. Cortical control of the autonomic nervous system. *Exp. Physiol.* **99**, 326–331 (2014).
32. Benarroch, E. E. The central autonomic network: functional organization, dysfunction, and perspective. *Mayo Clin. Proc.* **68**, 988–1001 (1993).
33. Schneebaum Sender, N. et al. Cerebral modulation of the autonomic nervous system in term infants. *J. Perinatol.* **37**, 558–562 (2017).
34. Schneebaum Sender, N. et al. Effects of regional brain injury on the newborn autonomic nervous system. *Early Hum. Dev.* **90**, 893–896 (2014).
35. Tasker, R. C. Intracranial pressure and cerebrovascular autoregulation in pediatric critical illness. *Semin Pediatr. Neurol.* **21**, 255–262 (2014).
36. Lowensohn, R. I., Weiss, M. & Hon, E. H. Heart-rate variability in brain-damaged adults. *Lancet* **1**, 626–628 (1977).
37. Oliveira, V. et al. Early postnatal heart rate variability in healthy newborn infants. *Front Physiol.* **10**, 922 (2019).
38. Sanderson, J. E. Limitations of heart rate variability measurements. *Am. J. Cardiol.* **74**, 417 (1994).
39. Alexander, A. L., Lee, J. E., Wu, Y. C. & Field, A. S. Comparison of diffusion tensor imaging measurements at 3.0 T versus 1.5 T with and without parallel imaging. *Neuroimaging Clin. N. Am.* **16**, 299–309 (2006).
40. Shaw, C. B., Jensen, J. H., Deardorff, R. L., Spampinato, M. V. & Helpert, J. A. Comparison of diffusion metrics obtained at 1.5t and 3t in human brain with diffusional kurtosis imaging. *J. Magn. Reson Imaging* **45**, 673–680 (2017).

ACKNOWLEDGEMENTS

We thank the children and their families for participating, Dr. Elana F. Pinchefskey and Dr. Carlos Ivan Salazar Cerda for their assistance with identification of seizure epochs.

AUTHOR CONTRIBUTIONS

I.G., Substantial contributions to conception and design, analysis and interpretation of data, drafting the manuscript; D.K., Substantial contributions to patient recruitment and data acquisition; E.W., Substantial contributions to interpretation and classification of neuroimaging; M.P., Substantial contributions to heart rate variability data analysis and interpretation; N.M., Substantial contributions to statistical analysis of the data; A.M., Conceptualization and conduct of the clinical trial, critical review of the manuscript; E.W.T., Substantial contributions to conception and design of the study, funding acquisition, critical review of the manuscript and final approval of the version to be published, Principal investigator and Supervisor to I.G.

FUNDING

This work was supported by research grants from the Canadian Institutes of Health Research [MOP-133710, PJT-166076], the National Institutes of Health [R01 HD101419], and SickKids Foundation awarded to EWYT.

CONSENT TO PARTICIPATE

Informed consent was taken from Parents of neonates enrolled in the study. The study was approved by local institutional ethics board.

COMPETING INTERESTS

The authors declare no competing interest.

ADDITIONAL INFORMATION

Supplementary information The online version contains supplementary material available at <https://doi.org/10.1038/s41390-022-02016-9>.

Correspondence and requests for materials should be addressed to Ipsita Goswami.

Reprints and permission information is available at <http://www.nature.com/reprints>

Publisher's note Springer Nature remains neutral with regard to jurisdictional claims in published maps and institutional affiliations.